

ENERGY DEPOSITION ISSUES AT 8 GeV H^- BEAM COLLIMATION AND INJECTION TO THE FERMILAB MAIN INJECTOR*

A.I. Drozhdin[†], M.A. Kostin, N.V. Mokhov, FNAL, Batavia, IL 60510, USA

Abstract

The energy deposition and radiation issues at 8 GeV H^- beam collimation in the beam transfer line and at stripping injection to the Fermilab Main Injector (MI) are analyzed. Detailed calculations with the STRUCT [1] and MARS 15 [2] codes are performed on heating of collimators and stripping foils, as well as on accelerator elements radioactivation at normal operation. Extraction of the unstripped part of the beam to the external beam dump and loss of the excited-state H^0 atoms in MI are also studied.

INTRODUCTION

Fermilab is currently working on the design of a superconducting RF linac, Proton Driver (PD). It will accelerate 1.5×10^{14} H^- ions up to 8 GeV with a total beam power of 0.5 MW upgradable to 2 MW. The H^- ions are stripped to protons in foils and injected into MI for acceleration to 32-120 GeV, mainly for neutrino oscillations studies. Results presented in this paper are for the 0.128 MW PD beam injected with the 0.67 Hz repetition rate into MI in the 120-GeV mode. The 32-GeV MI can be fed at 2.5 Hz by the 0.5 MW PD beam. The 8-GeV beam directly from PD can also be used for neutrino oscillation studies and other experiments. The energy deposition and radiation issues at 8 GeV H^- beam collimation in the beam transfer line and at stripping injection into MI are discussed below.

BEAM LINE COLLIMATION SYSTEM

The beam line is comprised of five sections (Fig. 1): beam matching between RF linac and the FODO lattice of beam line, amplitude collimation, momentum jitter correction and momentum collimation, matching between FODO lattice and MI. Halo collimation is done by stripping H^- ions at a foil located upstream of the focusing quadrupole and then intercepting H^0 atoms and protons at the beam dump located 5 m downstream of the focusing quadrupole (Fig. 1, bottom). Six foil-dump stations are used for amplitude collimation in the first three cells of the beam line, with two additional stations for momentum cleaning at locations with positive and negative dispersion wave maxima. Beam collimation is done at $3.5\sigma_{x,y}$ and $\Delta p/p = 0.001$.

As MARS15 calculations show (Fig. 2), the steel dump withstands, in principal, a single pulse of accidentally lost

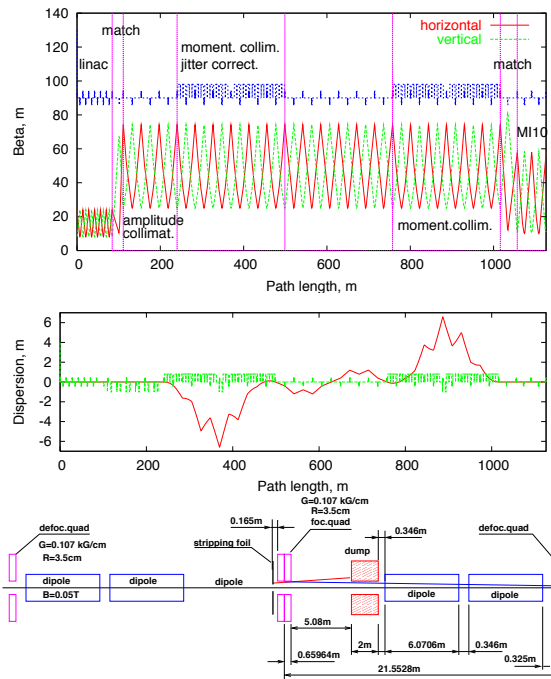


Figure 1: β functions (top), horizontal dispersion (middle) in the beam transfer line, and principal of stripping collimation (bottom).

beam but is melt if the next pulse arrives. If one assumes that the dump should withstand two pulses in a row, then the optimal solution would be a 0.5-m long and 10-mm radially thick graphite insert in a 1-m long steel dump.

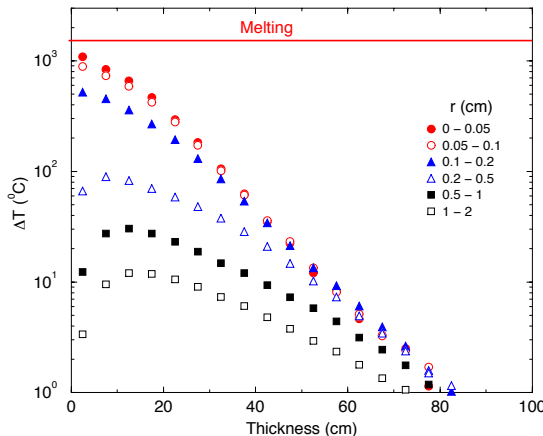


Figure 2: Instantaneous temperature rise in steel beam dump per a single pulse of 1.5×10^{14} protons at $\sigma_{x,y} = 1$ mm.

Total loss rate inside the bending magnet at H^- ion stripping from blackbody radiation, magnetic field and residual

* Work supported by the Universities Research Association, Inc., under contract DE-AC02-76CH03000 with the U. S. Department of Energy.

[†] drozhdin@fnal.gov

gas stripping is about 1.8×10^8 p/m or 0.15 W/m. We have found that with a tapered liner inside the bending magnets at 2 m to their downstream ends, irradiation of the interconnect regions can be reduced by an orders of magnitude down to about 0.5 mSv/hr.

PAINTING INJECTION

Painting injection of the 8-GeV H^- beam is performed by using four horizontal kicker magnets in MI and two pairs of the horizontal and vertical kicker magnets located in the injection beam line (Fig. 3). Gradual reduction of the kicker strengths allows “painting” of the injected beam across the aperture to the required emittance.

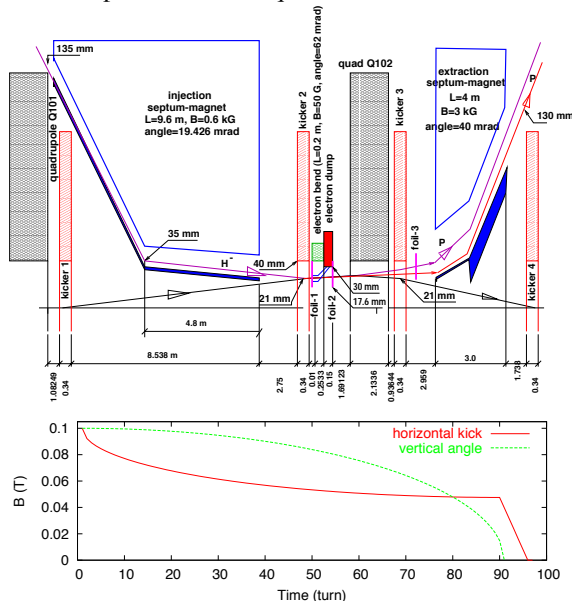


Figure 3: Painting injection scheme (top) and kicker strength during injection (bottom).

The stripping foil is located at the exit of the second painting kicker in its fringe field. The kicker magnet field is chosen such that it provides stripping of atoms with principal quantum numbers $n \geq 5$. As shown in Fig. 4, this requires the kicker field to be ≥ 0.05 T. From the other hand, the field should be low enough to minimize the H^- ions stripping. It is seen from Fig. 3 that the kicker strength decreases from 0.1 T to 0.06 T during 20 turns, and then slowly drops to 0.05 T during another 70 turns. Estimations show that at the beginning of injection the magnetic field of the second kicker causes stripping of 5×10^{-5} of injected H^- , producing 7 W of power loss downstream the foil. The stripping probabilities of H^0 Stark state hydrogen atoms in downstream magnets are presented in Table 1. It is assumed here that H^0 atoms pass a distance of ~ 1 cm in the maximum fringe field of the kicker magnet. This distance is enough for H^0 atoms with $n \geq 5$ to be stripped to protons, which go to the circulating beam without changing the beam emittance. Some atoms with $n=4$ are left unstripped and go to the beam dump, and, unfortunately, some fraction of them is stripped in the third kicker. These pro-

tons will contribute to the circulating beam halo and cause losses downstream of the kicker.

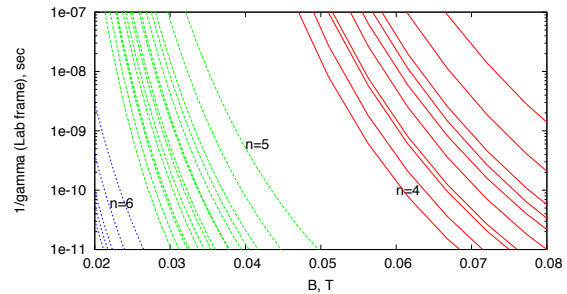


Figure 4: Calculated lifetime of Stark state 8-GeV hydrogen atoms in magnetic field.

Table 1: A stripping probability of 8 GeV H^0 Stark state hydrogen atoms.

n	lifetime		decay length	effect
	B	sec		
kicker No.2, $L_{field} \approx 1$ cm				
4	0.1	$< 10^{-11}$	0.003	stripped
4	0.06	$> 10^{-10}$	0.03	unstripped
5	0.06	$< 10^{-12}$	0.0003	stripped
4	0.05	$> 10^{-8}$	3.0	unstripped
5	0.05	$< 10^{-11}$	0.003	stripped
quadrupole Q102, $L_{field} = 2.1$ m				
4	0.025	> 100		unstripped
kicker No.3, $L_{field} = 0.34$ m				
4	0.1	$< 10^{-10}$	0.03	stripped
4	0.06	$10^{-10} - 10^{-6}$	0.03 - 300	partial stripped
4	0.05	$10^{-8} - 10^{-4}$	3 - 30000	unstripped

The circulating protons pass several times through the foil. Multiple Coulomb scattering is small because of small foil thickness. Particle ionization loss in the foil at one pass is $4 \cdot 10^{-20}$ of initial energy. Multi-turn simulations show that 0.03% of the injected beam is lost in the accelerator because of nuclear and elastic interactions in the foils for the 270-turn injection. This fraction is a factor of three less for the 90-turn one.

HEATING AND RADIOACTIVATION

Two carbon stripping foils $1.5 \mu\text{m}$ thick ($300 \mu\text{g}/\text{cm}^2$) with a transverse size of $12 \times 12 \text{ mm}^2$ are located 0.4 m apart. Protons pass through the foils 4.4 and 15.9 times on average at the 90 and 270-turn injections, respectively. This includes the very first pass while the protons are still constituents of H^- ions. It is assumed that the energy deposition is instantaneous and there is no evolution of the foil temperature during the injection. Most of the H^- ions are stripped in the first foil and the electrons are removed before the second foil. The foil heating calculations with the MARS15 code were done with a conservative assumption that all the H^- ions were stripped in the very upstream part of the first foil and electrons passed through it contributing to the heating. At the same time, it was assumed that 20% of H^- ions survive the first foil and are

stripped in the second foil. The proton energy of 8 GeV corresponds to a Lorentz-factor of 9.526 and the electron energy of 4.357 MeV. As shown in Table 2, the instantaneous temperature rise for the 270-turn injection is close to the carbon integrity limit. Fig. 5 is a graphical representation of the temperature rise after one cycle of 270-turn injection.

Table 2: Energy deposition and instantaneous temperature rise in the stripping foils due to electrons, protons and both.

	Peak energy deposit		Peak temperature rise	
	Foil 1	Foil 2	Foil 1	Foil 2
	J/g		K	
Electron	1478	296	-	-
Proton, 90-turn	2182	2230	-	-
Proton, 270-turn	6616	6639	-	-
e + p, 90-turn	3621	2502	1991	1470
e + p, 270-turn	6616	6639	3358	3368

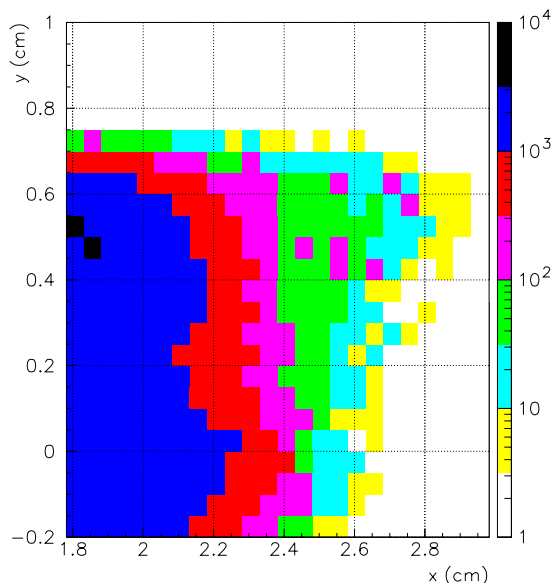


Figure 5: Instantaneous temperature rise in the first stripping foil for the 270-turn injection.

Residual dose on the upstream end of the hottest quadrupole beyond the foil after 30 days of irradiation and 1 day of cooling, also known as a “0 cm/30 days/1 day” dose, varies from 20 mSv/hr down to 0.1 mSv/hr for the 90-turn injection and from 74 mSv/hr to 0.1 mSv/hr for the 270-turn one (1 mSv = 100 mrem). A corresponding 2D distribution is shown in Fig. 6. Table 3 summarizes the averaged residual doses on the quadrupole surface.

Table 3: Residual dose on six surfaces of the hottest quadrupole.

Surface	Residual dose (mSv/hr)	
	90-turn inject.	270-turn inject.
front	4.1	15.5
rear	0.16	0.57
left	0.15	0.69
right	0.22	0.77
bottom	0.41	1.41
top	0.46	1.63

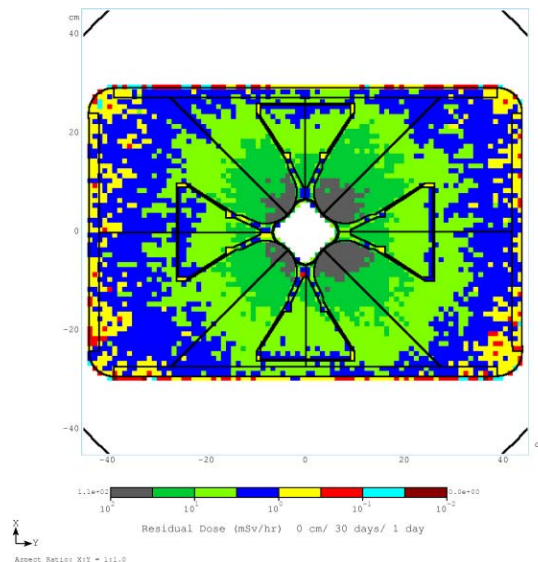


Figure 6: Residual dose on the upstream end of the first quadrupole downstream the foil for the 270-turn injection.

The most radiation-sensitive magnet ingredients are epoxy and coil insulation. A typical lifetime limit on the absorbed dose for these materials is about 4 MGy (1 MGy = 100 Mrad). The MARS-calculated peak absorbed dose in the quadrupole coils is about 1 MGy/yr that corresponds to about 4-year lifetime.

INJECTION BEAM DUMP

The H^0 atoms remaining after the stripping injection are directed to an additional thick foil to ensure a complete stripping to protons before extracting them to an external beam dump. As a real stripping efficiency is unknown, we follow a conservative approach allowing up to 10 kW of beam power to be absorbed by the beam dump. This corresponds to 8% of the injected beam directed to the dump. A shutdown after a beam accident will allow to investigate the cause of the accident and to keep an integrated particle rate on the beam dump in a required limits.

The design goal for the injection beam dump is to achieve similar radiation level as at the existing MI beam dump which consists of a $0.15 \times 0.15 \times 2.4$ -m graphite core, a 0.15-m thick aluminum water-cooled box, surrounded by a 0.84-m steel followed by 1.1-m concrete shielding. The MARS15 calculations show that additional 0.3 m of steel shielding is needed in order to achieve the design goals.

REFERENCES

- [1] A.I. Drozhdin, et al. “STRUCT Program User’s Reference Manual”, <http://www-ap.fnal.gov/users/drozhdin/>
- [2] N.V. Mokhov, “The MARS Code System User’s Guide”, Fermilab-FN-628 (1995); N.V. Mokhov, et al, “Recent Enhancements to the MARS15 Code”, Fermilab-Conf-04/053 (2004); <http://www-ap.fnal.gov/MARS/>.